

# **FINITE ELEMENT SIMULATIONS OF BLAST LOADING ON SANDWICH STRUCTURE**

**M.Tech Thesis**

by

**Mahima Yadav**



**DISCIPLINE OF MECHANICAL ENGINEERING  
INDIAN INSTITUTE OF TECHNOLOGY INDORE**

**JUNE 2024**

# **FINITE ELEMENT SIMULATIONS OF BLAST LOADING ON SANDWICH STRUCTURE**

**A THESIS**

*Submitted in partial fulfillment of the  
requirements for the award of the degree*

*of*

**Master of Technology**

*by*

**Mahima Yadav**



**DISCIPLINE OF MECHANICAL ENGINEERING  
INDIAN INSTITUTE OF TECHNOLOGY INDORE**

**JUNE 2024**



# INDIAN INSTITUTE OF TECHNOLOGY INDORE

## CANDIDATE'S DECLARATION

I hereby certify that the work which is being presented in the thesis entitled **FINITE ELEMENT SIMULATIONS OF BLAST LOADING ON SANDWICH STRUCTURE** in the partial fulfillment of the requirements for the award of the degree of **MASTER OF TECHNOLOGY** and submitted in the **DISCIPLINE OF MECHANICAL ENGINEERING, Indian Institute of Technology Indore**, is an authentic record of my own work carried out during the time period from July 2022 to June 2024. Thesis submission under the supervision of **Dr. Indrasen Singh**, Assistant Professor in Mechanical Engineering, Indian Institute of Technology Indore.

The matter presented in this thesis has not been submitted by me for the award of any other degree of this or any other institute.

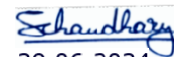
  
28/6/2024

**Mahima Yadav**  
**(M.Tech. Student)**

-----  
This is to certify that the above statement made by the candidate is correct to the best of my/our knowledge.

  
29-06-2024

**Dr. Indrasen Singh**  
**(Thesis Supervisor 1)**

  
29.06.2024

**Prof. Sandeep Chaudhary**  
**(Thesis Supervisor 2)**

-----  
**Mahima Yadav** has successfully given his M.Tech. Oral Examination held on **30 May 2024**.

  
29-06-2024

Signature of Supervisors of M.Tech. thesis

Date:



Convener, DPGC

Date: 01-07-2024

## **ACKNOWLEDGEMENTS**

I would like to express my deepest gratitude to everyone who contributed to the completion of this project. First and foremost, I am incredibly grateful to Dr. Indrasen Singh, my advisor, for their valuable guidance, constant support, and insightful feedback throughout this research. Their expertise and encouragement have been instrumental in shaping this work, their training that I got throughout this project will definitely help me a lot in the corporate world. I would also like to extend my heartfelt thanks to IIT Indore for providing the necessary resources and facilities to conduct this study. Special thanks to my colleague and best friend Mr. Rohan Dewda who always helped me with making different structures and always kept me motivated throughout this journey. I am thankful to all my lab mates and a special thanks to Mr. Ramanand Dadhich and Mr. Sumit Chorma for their constant encouragement and help throughout my tenure in this project.

A special mention goes to my grandfather Mr. Kamal Yadav and Grandmother Mrs. Nanda Yadav for their love and constant motivation at my low's. Their belief in me has been a source of strength and motivation. I also want to express my deep gratitude towards my whole family for always being there for me.

Thank you all for your contributions, without which this work would not have been possible.

**Dedicated to my grandparents**

**Mr. Kamal Yadav and Mrs. Nanda Yadav**

## ABSTRACT

The threat posed by terrorist activities and explosive devices necessitates the continuous evolution of protective technologies, including blast-resistant materials and structures. Specifically, in the context of footwear for soldiers exposed to the risks of landmines and other explosive devices, optimizing blast-resistant sandwich structures is crucial. These structures typically consist of layered compositions designed to absorb shock waves and attenuate pressure generated by explosions. The core materials used in these structures are, generally, honeycomb, and auxetic/meta-structured cores which offer distinct advantages in terms of energy absorption and structural stability. Among the various cores, honeycomb have gathered attention for blast loading due their high energy absorption characteristics. There are various length scales associated in these honeycomb such as cell wall thickness, cell size. In addition, the loading orientations (in-plane and out-of-plane) has also shown to influence the energy absorption greatly. In order to determine, the optimum shape, size and loading direction for specific loading conditions, a detailed study is needed. There are few studies undertaken in this direction, but a very little efforts has been made to understand the deformation behavior of sandwich structure subjected to near-field blast. Therefore, continuum simulations of near-field blast loading have been undertaken in this study. Results shows that thinner shells are better in attenuating pressure but in turn absorbs lesser energy hence optimum thickness is found, further the decrease in cell size leads to greater energy absorption and effective pressure attenuation capability, additionally it is found that the combination of square out-of-plane honeycomb and auxetic in-plane honeycomb cores shows better blast resistance than structures with only in-plane auxetic honeycomb cores, in terms of both energy absorption and pressure attenuation, specifically when the in-plane auxetic honeycomb core is placed on the blast side.

# TABLE OF CONTENTS

|    |   |     |
|----|---|-----|
| 1. | <b>LIST OF FIGURES</b> .....                                  | vii |
| 2. | <b>LIST OF TABLES</b> .....                                   | ix  |
| 3. | <b>NOMENCLATURE</b> .....                                     | x   |
| 4. | <b>ACRONYMS</b> .....   | xi  |
| 5. | <b>Chapter 1: Introduction and literature review</b> .....    | 1   |
|    | 1.1 Introduction.....   | 1   |
|    | 1.2 Sandwich structure.....                                   | 1   |
|    | 1.2.1 Cellular Foam Core .....                                | 2   |
|    | 1.2.2 Honeycomb Core Structure.....                           | 3   |
|    | 1.2.3 Auxetic Core Structure.....                             | 4   |
|    | 1.3 Materials for different layers in sandwich structure..... | 4   |
|    | 1.4 Literature Review.....                                    | 4   |
|    | 1.5 Research gap.....   | 5   |
|    | 1.6 Objectives.....   | 6   |
|    | 1.7 Organization of the Thesis.....                           | 6   |
| 6. | <b>Chapter 2: Finite Element Simulations</b> .....            | 8   |
|    | 2.1 Material models.....                                      | 8   |
|    | 2.1.1 Johnson Cook Plasticity Model.....                      | 8   |
|    | 2.1.2 Johnson Cook damage Model.....                          | 9   |
|    | 2.1.3 Mohr coulomb plasticity.....                            | 10  |
|    | 2.1.4 Equation of state .....                                 | 10  |
|    | 2.2 Finite element (FE) model .....                           | 11  |
|    | 2.2.1 Eulerian Domain and Discretization.....                 | 11  |

|       |  |           |
|-------|--|-----------|
| 2.2.2 | Material distribution.....                         | 12        |
| 2.2.3 | Explosive and Structure Placement.....             | 12        |
| 2.2.4 | Boundary Conditions.....                           | 12        |
| 2.2.5 | FEM model of sandwich structure.....               | 13        |
| 2.3   | Material parameters.....                           | 16        |
| 7.    | <b>Chapter 3: Result and discussion.....</b>       | <b>18</b> |
| 3.1   | Effect of cell wall thickness.....                 | 18        |
| 3.2   | Effect of cell size.....                           | 18        |
| 3.3   | Effect of combining in plane and out of plane..... | 21        |
| 8.    | <b>Chapter 4: Conclusion and future scope.....</b> | <b>24</b> |
| 4.1   | Conclusion.....                                    | 24        |
| 4.2   | Future scope of work.....                          | 24        |
| 9.    | <b>References .....</b>                            | <b>25</b> |

## LIST OF FIGURES

|     |   |    |
|-----|---|----|
| 1.  | Fig. 1.1 Schematic of sandwich structure.....   | 2  |
| 2.  | Fig. 1.2 Typical image of cellular foam core.....   | 2  |
| 3.  | Fig. 1.3 Sandwich structure with honeycomb core.....  | 3  |
| 4.  | Fig. 1.4 Different types of auxetic structures used as core in sandwich structure.....  | 3  |
| 5.  | Fig. 1.5 Different shoes under blast loading and their response.....  | 6  |
| 6.  | Fig. 2.1 Typical stress-strain diagram of ductile materials.....  | 9  |
| 7.  | Fig. 2.2 Modelling strategy (a) Schematic of assembly for finite element simulation, (b) Abaqus Model.....                                      | 11 |
| 8.  | Fig. 2.3 Boundary conditions of (a) Domain, (b) Structure.....  | 12 |
| 9.  | Fig. 2.4 Blast resistant auxetic honeycomb structure.....   | 13 |
| 10. | Fig 2.5 Finite element model of auxetic honeycomb structure employed in the simulations of blast loading.....                                   | 14 |
| 11. | Fig. 2.6 Finite element model of domain employed in the simulations of blast loading .....  | 14 |
| 12. | Fig. 2.7 Variation of cell wall thickness.....  | 15 |
| 13. | Fig 2.8 Varying the size of cell of an auxetic honeycomb (a) 24 mm, (b) 12 mm, (c) 6 mm.....  | 15 |
| 14. | Fig 2.9 Different configurations of in-plane and out-of-plane honeycomb structure (a) Out-of-plane facing blast, (b) in-plane facing blast..... | 16 |
| 15. | Fig. 3.1 Evolution of damage for different cell wall thickness structures ....  | 18 |
| 16. | Fig. 3.2 Evolution of energy absorption for different cell wall thickness.....  | 19 |
| 17. | Fig. 3.3 Evolution of pressure on the top surface of structure for different cell wall thicknesses.....   | 19 |
| 18. | Fig. 3.4 Contour plots of equivalent plastic strain for different cell size; (a) 24 mm, (b) 12 mm, (c) 6 mm.....                                | 20 |

|     |   |    |
|-----|---|----|
| 19. | <b>Fig. 3.5</b> Evolution of energy absorption for different cell size honeycomb structures.....  | 20 |
| 20. | <b>Fig. 3.6</b> Evolution of pressure on the top surface for different cell size honeycomb structures.....  | 21 |
| 21. | <b>Fig. 3.7</b> Contour plots of equivalent plastic strain for (a) In-plane honeycomb on blast side, (b) Out-plane honeycomb on the blast side..... | 22 |
| 22. | <b>Fig. 3.8</b> Energy absorption for in plane and out of plane combined with one of them facing blast side.....                                    | 22 |
| 23. | <b>Fig. 3.9</b> Pressure variation for in plane and out of plane combined with one of them facing blast side.....                                   | 23 |

## LIST OF TABLES

|    |  |    |
|----|--|----|
| 1. | Table. 1 Material properties for air.....      | 16 |
| 2. | Table. 2 Material properties for soil.....     | 16 |
| 3. | Table. 3 Material properties for TNT.....      | 17 |
| 4. | Table. 4 Material properties for aluminum..... | 17 |

# NOMENCLATURE

## Symbols

|           |                                     |
|-----------|-------------------------------------|
| $A$       | Yield stress                        |
| $B$       | Work hardening coefficient          |
| $C$       | Strain rate sensitivity coefficient |
| $D$       | Damage parameter                    |
| $\dot{D}$ | Rate of damage                      |
| $n$       | Work hardening exponent             |
| $m$       | Thermal softening exponent          |
| $T$       | Actual temperature                  |
| $T_r$     | Room temperature                    |
| $T_m$     | Melting temperature                 |
| $W$       | Mass of TNT                         |

## Greek letters

|                     |                                 |
|---------------------|---------------------------------|
| $\omega$            | State variable                  |
| $L_{eq}$            | Characteristic length           |
| $\underline{u}_f^p$ | Plastic displacement at failure |
| $\eta$              | Triaxiality                     |

|                    |                           |
|--------------------|---------------------------|
| $\epsilon_f^p$     | Plastic strain at failure |
| $\sigma_{eq}$      | Equivalent stress         |
| $\epsilon_p$       | Equivalent plastic strain |
| $\dot{\epsilon}_p$ | Strain rate               |
| $\dot{\epsilon}_0$ | reference strain rate     |

# ACRONYMS

|        |  |
|--------|--|
| CONWEP | Conventional Weapon Method                       |
| SPH    | Smooth Particle Hydrodynamics                    |
| CEL    | Coupled Eulerian Lagrangian                      |
| EOS    | Equation of State                                |
| TNT    | Trinitrotoluene                                  |
| JWL    | Jones-Wilkins-Lee                                |
| FE     | Finite Element                                   |
| BAMI   | Boot Anti Mine Infantry                          |
| EC3D8R | Explicit Continuum 3D 8-node Reduced Integration |
| C3D8R  | Continuum 3D 8-node Reduced Integration          |
| S4R    | Shell 4-node Reduced Integration                 |

# Chapter 1

## Introduction and literature review

### 1.1 Introduction

Increasing terrorist activities is a biggest threat for our country nowadays, which is causing numerous fatalities. In order to avoid the threat caused by blast or to mitigate the effects of blast, the blast resistant structure plays a vital role. These specialized structures are design to withstand very high rate of loading and absorb shock waves and attenuate pressure generated by sudden blast. In recent years, research on the blast protective structures has gain a lot of popularity.

Blast loads are categorized as far field and near field blast which is differentiated by a criterion known as scaled distance. Both of these fields are associated with explosions that occur at scaled distance of more or less than 1.18. This far field and near field not only depend on the distance of explosive from the system but it also depends on amount of explosive. Generally, explosives are buried around 25 – 50 mm below the ground in land mines. The aim of this study is to design specialized shoes for soldiers to mitigate blast effects and minimize injuries. This problem comes under near field blast as this kind of blast where the system which needs to be analyzed is in very close proximity to landmines. Therefore, the objective of the present study is to design the blast resistant shoe in order to avoid the injuries and fatalities caused by the landmine blast. This can be done by using the sandwich structure in the shoe sole. The optimization of structure is needed in order to increase its specific energy absorption and reduce peak pressure transmitted which is in direct contact with the human leg. A brief description of sandwich structure and its types and material used is given below.

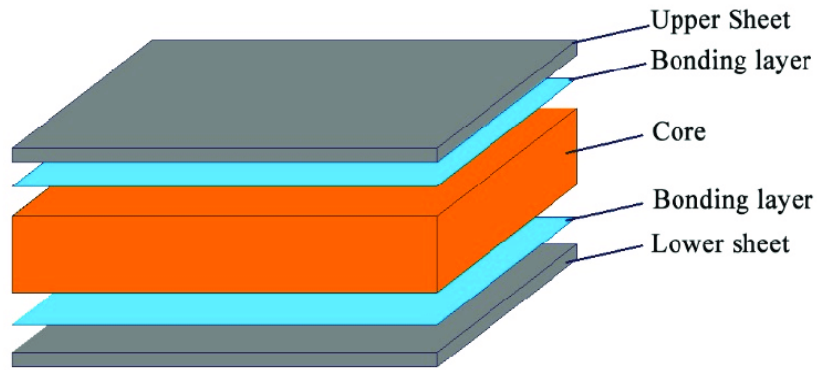
### 1.2 Sandwich structure

Fig. 1.1 shows a sandwich structure which comprises of three layers, namely two slender, robust face sheets and a thick, lightweight core. The core material assumes a critical role in conferring distinctive mechanical properties to the structure, the components of the sandwich structure are as follows:

**Face Sheets:** Typically composed of metals (such as aluminum, steel), fiber-reinforced polymers (like carbon fiber, fiberglass), or other resilient materials. These layers primarily endure most of the in-plane loads, offer structural stiffness, and safeguard the core.

**Core:** The core is engineered to absorb impact energy, deliver thermal insulation, and uphold the separation between the face sheets , thereby augmenting the overall rigidity and durability of the sandwich structure.

Various materials can be utilized for the core, including foams (metallic or polymeric), honeycomb configurations, and auxetic/meta-structured materials. These are summarized in the following.



**Fig. 1.1** Schematic of sandwich structure taken from [1].

There are several types of cores being used in sandwich structure. The most common one are discussed below:

### 1.2.1 Cellular foam core structure

The typical schematic of cellular foam structure is given in Fig 1.2. Foams absorb significant energy during plastic deformation, with a typical plateau covering 60-70% of the strain. Their properties depend heavily on density, which allows for customized designs, and they can be open-cell or closed-cell. The cellular foams can be made up of either metals or polymers. The polymeric foam provides decent strength to weight ratio, and also prevent heat reaching the foot of the personnel, while metallic foams provide very high strength to weight ratio and are utilized for superior energy absorption, including low-velocity impacts [2] and crashworthiness [3].

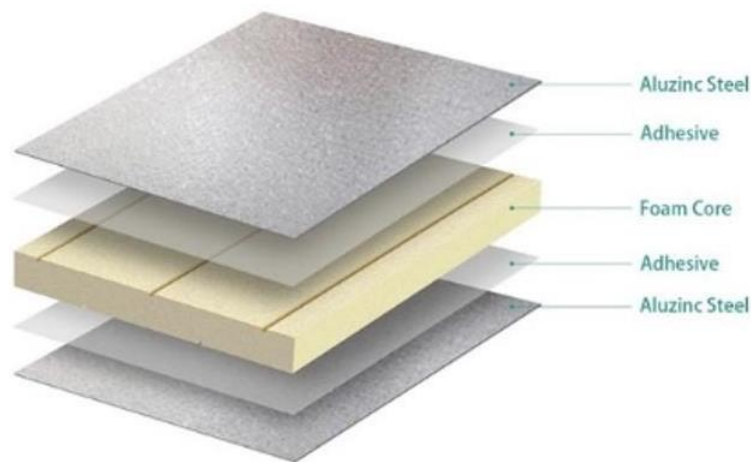


**Fig. 1.2** Typical image of cellular foam core [4].

### 1.2.2 Honeycomb structure:

The honeycomb structure (refer Fig. 1.3) consist of cells of different shape, size, and orientation, they are employed for low-velocity impact [5], shockwave [6], blast loading [7, 8], and crashworthiness [9]. Multiple layered honeycomb sandwiched structures, also known as graded honeycomb structures have also been used in the application of blast resistant structure. The geometric parameters like cell wall thickness, cell size, face sheet thickness plays important role for the performance of the structure and hence structure can be customized for the particular application by tailoring the values of the various geometric parameters.

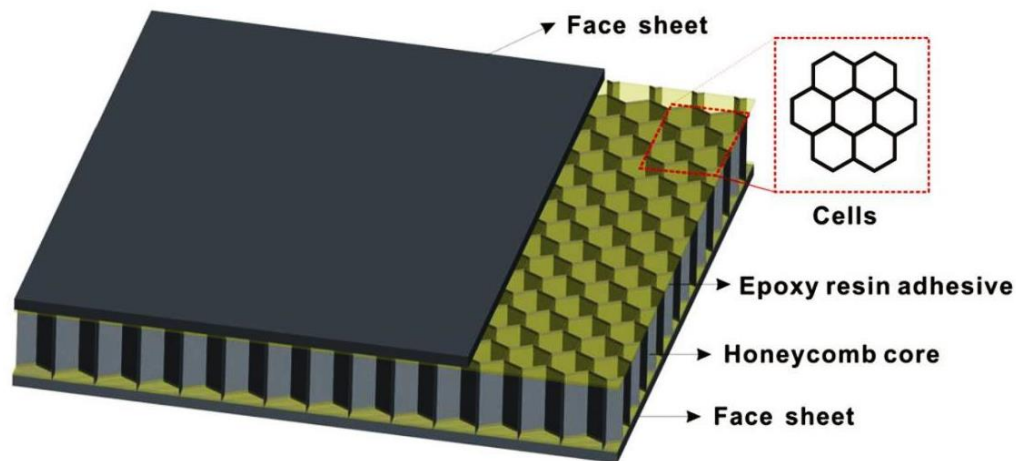


Fig. 1.3 Sandwich structure with honeycomb core [10].

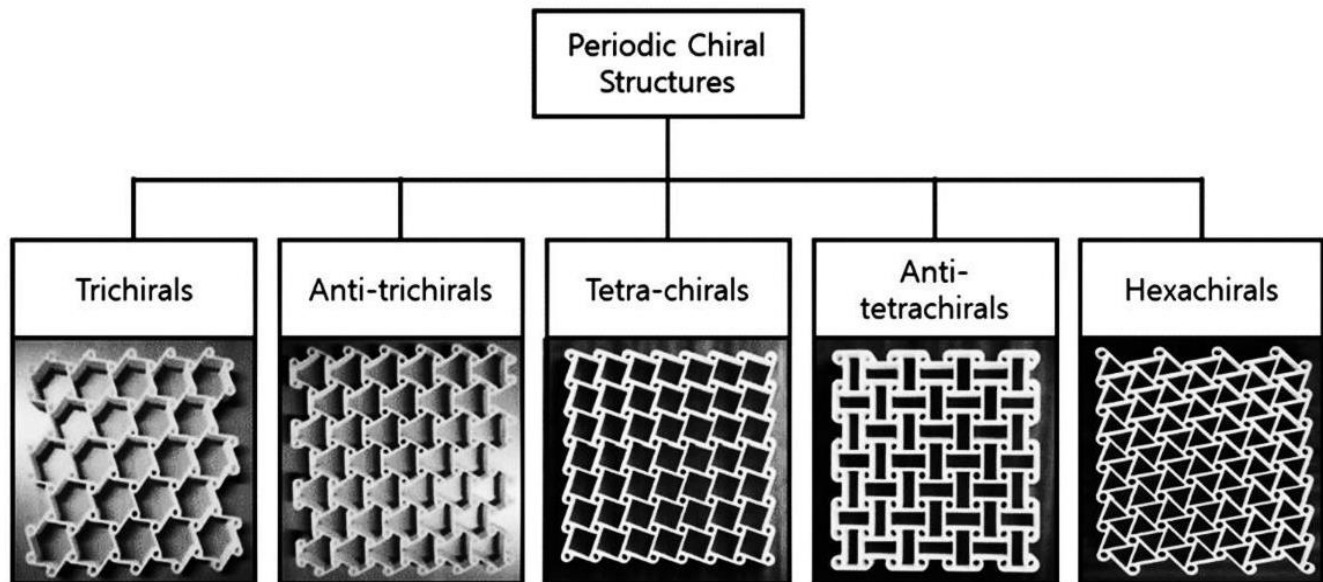


Fig. 1.4 Different types of auxetic structures used as core in sandwich structure [12].

### 1.2.3 Auxetic core structures

The typical schematic of auxetic structure is given in Fig. 1.4. Auxetic structures, are the structures with a negative Poisson's ratio and are very effective under dynamic loading conditions, the property of possessing negative Poisson's ratio enables auxetic structures to deform laterally when compressive load is applied in transverse direction, leading to uniform deformation throughout the cross-section, thus enhancing energy absorption and are therefore found to be superior than regular hexagonal honeycomb structures [11].

### **1.3 Materials for different layers in sandwich structure**

In blast-resistant sandwich structures, particularly those designed for protection against explosive threats like landmines, the choice of materials for each layer plays a critical role in determining the overall performance and effectiveness of the structure. The bottom face sheet, which directly faces the blast side, is typically composed of materials known for their high strength and ability to withstand sudden impact and fragmentation. Ceramic materials are commonly used due to their exceptional hardness, stiffness, and resistance to penetration [13], some examples are alumina or boron carbide [13]. Ceramics are advantageous in blast scenarios because they can absorb and distribute impact energy effectively, thereby reducing the transmission of damaging forces to the core and the occupant. Kevlar is a strong synthetic fiber that is known for its high tensile strength and resistance to abrasion, it is often integrated into composite structures with ceramics [14]. Kevlar fibers can significantly enhance the toughness and impact resistance of the face sheet, providing additional protection against ballistic and blast threats [15].

Now coming to the core material of the sandwich structure, aluminum is frequently used for its favorable combination of properties, including lightweight, high strength-to-weight ratio, and good energy absorption capabilities. In blast scenarios, aluminum cores can deform plastically to absorb significant amounts of energy, thus mitigating the impact on the protected area. This deformation process helps in dissipating the blast energy and reducing the transmission of damaging forces to the occupant or sensitive equipment within the structure.

In summary, the combination of ceramic and Kevlar in the face sheet, along with aluminum in the core of blast-resistant sandwich structures, represents a balanced approach to enhancing protection against explosive threats.

### **1.4 Literature review**

The dynamic response of sandwich structures under blast conditions has been a focal point of research, as evidenced by the work of Dharmasena et al. [7]. Their explosive tests on square honeycomb core sandwich panels and solid panels revealed that honeycomb sandwich panels produce smaller back face deflections

compared to solid plates of identical mass. This finding highlights the superior blast mitigation capabilities of honeycomb structures, particularly in reducing back face deformation. Building on this, further studies have demonstrated the impact of face sheet thickness on the performance of both metallic foam and honeycomb core panels [16]. Increased thickness of the face sheet has been noted to enhance the blast resistance capacity and if they are paired with honeycomb cores, they are known to increase the blast resistance capacity of the structure remarkably [16]. The exploration of out-of-plane ballistic impact behavior has also been investigated by Thomas et al. [8], particularly due to the exceptional energy absorption properties of honeycombs in this orientation. This is crucial for applications such as vehicle armor and aircraft panels, where multidirectional loads are common [17,18]. However, these applications also introduce complexity, as the structures must effectively handle varying impact directions.

Increasing cell-wall thickness and node length enhanced resistance, while larger cell sizes tended to reduce it [8, 19]. Finite Element Method (FEM) simulations, using models such as the Johnson Cook model for steels and the Ogden model for low-density closed-cell polyurethane (PU) foams, have closely matched experimental results. These simulations revealed that foam filling, depending on the thickness of face and corrugated sheets as well as boundary conditions, can significantly reduce front face deflections. However, increasing the thickness of these sheets can diminish the benefits of foam filling. Additionally, research has shown that constrained boundary conditions [20-22] result in lower front face deflections in comparison to the simply supported conditions. Another promising development is the use of auxetic cores, which are known to improve the blast resistance of sandwich plates, has been presented by Michalski et al. [23]. The utilization of auxetic cores results in decrease in total displacement and stress under blast conditions. Studies focusing on graded auxetic honeycomb cores have emphasized their dynamic behavior under external blast forces. These studies demonstrate that the orientation of these structures plays a significant role in enhancing resistance to deformation and energy absorption under compressive stresses [24, 25]. Moreover, research has delved into the design of protective boots with varying sole configurations to absorb energy from blasts. Comparisons between protective boots with reinforced soles and standard-issue military boots have shown that incorporating glass microspheres significantly enhances energy absorption. Protective boots, which feature glass microspheres, provide comprehensive defense against a 70g TNT impact as can be seen in Fig. 1.5, with a marked reduction in strain values compared to other designs [26].

## **1.5 Research gap**

Current research on sandwich structures and their response to ballistic impact and blast loading highlights several areas that require further investigation. Although various studies have been focused to find the effects of different geometrical parameters of sandwich structure on the overall performance of the

structure under far field blast loading. However, a few studies are focused on understanding the effects of geometrical parameters of sandwich structure on the performance of structure subjected to near field blast loading conditions. The existing literature falls short in exploring the application of a hybrid combination of in-plane and out-of-plane honeycomb structure included in a single structure exposed to near-field blast loads. Such an approach holds promise for harnessing the advantages of both types of honeycombs: the rigidity offered by out-of-plane configurations and the flexibility characteristic of in-plane honeycombs.

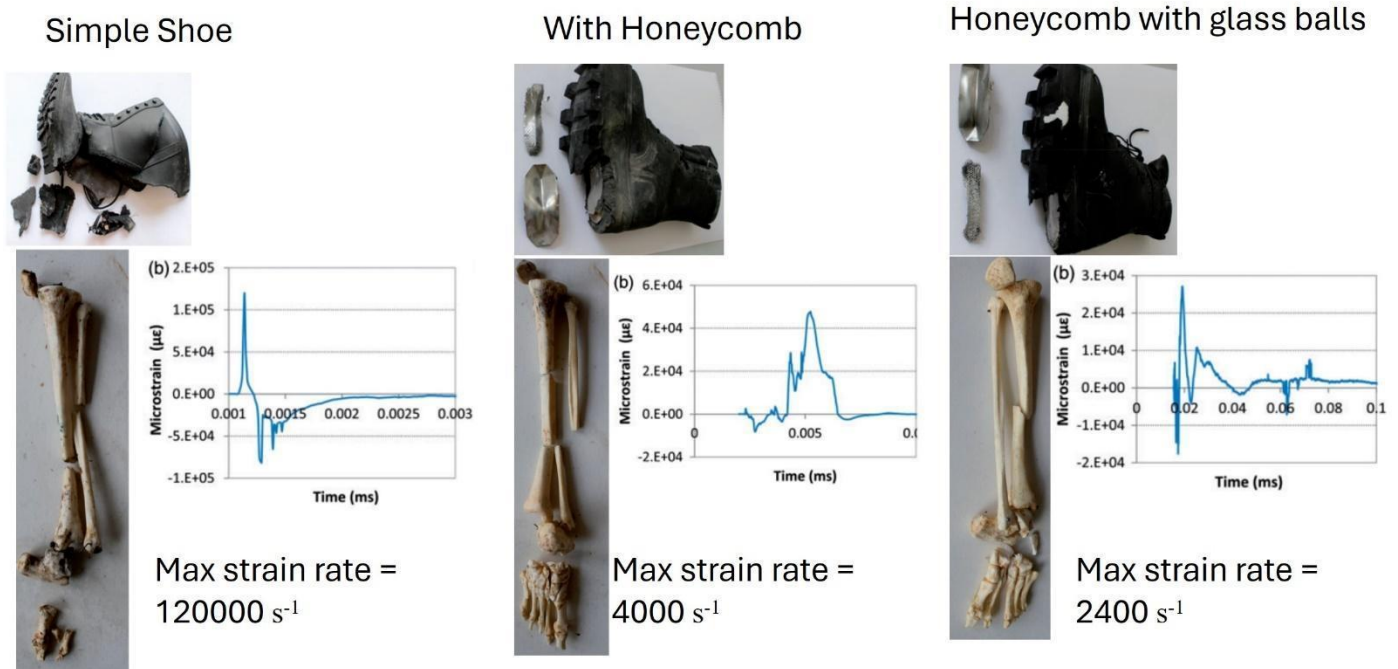


**Fig. 1.5** Different shoes under blast loading and their response [26]

## 1.6 Objectives

To perform finite element simulation of near field blast loading on sandwich structures consisting of auxetic honeycomb as a core. The thesis focuses on investigating the effect of variation of cell wall thickness, variation of cell size, and to find the effect of hybrid combination of in-plane and out-of-plane honeycomb structures subjected to near field blast loading conditions. Additionally the effect of order of in-plane and out-of-plane honeycombs within the structure is also investigated.

## 1.7 Thesis organization

This thesis contains four chapters, and a small brief idea has been given about the following:

### Chapter 2. Finite element simulations:

Different methods have been described in order to carry out the simulations and the best method has been picked to do the simulation of near field with reduced errors chances. Description of Development of a FE 3D and modelling strategies have been discussed.

### **Chapter 3. Results and discussion:**

Results of the different variations made in auxetic structure have been shown in this section and different energy absorption and peak pressure graphs have been discussed.

### **Chapter 4. Conclusion and future scope:**

In this part of the thesis the conclusion of the investigation on auxetic sandwich structure has been summarized and future work scopes have been discussed.

## Chapter 2

### Finite Element Simulations

Various numerical methods are utilized in the simulation of blast events, depending on the specific scenario and materials involved. The conventional weapon method (CONWEP method), a commonly employed approach, is well-suited for modeling air blast scenarios in far-field conditions by approximating blast events through incident and reflected pressure waves. This method offers a simplified yet effective way to simulate the impact of explosives on structures.

Smooth Particle Hydrodynamics (SPH) provides a meshless numerical technique that represents bodies through discrete points, allowing for detailed simulations of fluid dynamics and material interactions. SPH is particularly beneficial in scenarios requiring accurate depiction of complex fluid-structure interactions, making it a versatile option for simulating blast waves and their effects on structures.

The Coupled Eulerian-Lagrangian (CEL) method combines Lagrangian representation for structures with Eulerian representation for surrounding materials like soil, explosives, and air. This approach is well-suited for modeling detonation phenomena using equations of state, enabling detailed simulations of structural deformation and responses to blast loading conditions. The CEL approach has been selected for this study to simulate how structures deform under blast loading, offering insights into the performance of different materials and designs when faced with explosive threats.

## 2.1 Material models

### 2.1.1 Johnson Cook plasticity model

The plastic flow of the Aluminum honeycomb is assumed to follow the Johnson Cook law to incorporate the effect of strain hardening and strain rate hardening. The key equations of the Johnson Cook Model are shown below.

$$\sigma_{eq} = [A + B \epsilon_p^n] \times \left[1 + C \ln\left(\frac{\dot{\epsilon}_p}{\dot{\epsilon}_0}\right)\right] \times \left[1 - \left(\frac{T - T_r}{T_m - T_r}\right)^m\right]. \quad (2.1)$$

here,  $\epsilon_p$  is equivalent plastic strain,  $\dot{\epsilon}_p$  is plastic strain rate, and  $\dot{\epsilon}_0$  is reference strain rate. Further,  $T$ ,  $T_r$ , and  $T_m$  represent actual temperature, room temperature and melting temperature, respectively. Moreover,  $\sigma_{eq}$  is flow stress, while A, B and C are yield strength of the material, work hardening coefficient and strain

rate sensitivity respectively. Further, the constants  $n$  and  $m$  represent work hardening exponent and thermal softening coefficient, respectively.

### 2.1.2 Johnson Cook damage model

To simulate the failure of the honeycomb structure, the damage model of Johnson Cook (refer Fig. 2.10) this is given by the following equations.

$$\epsilon_f^p = [D_1 + D_2 e^{-D_3 \eta}] \times \left[ 1 + D_4 \ln \ln \left( \frac{\epsilon_p}{\epsilon_0} \right) \right] \times \left[ 1 + D_5 \left( \frac{T - T_r}{T_m - T_r} \right) \right], \quad (2.2)$$

here,  $D_1 - D_5$  are damage parameters, while  $\epsilon_f^p$  is equivalent failure strain. Further,  $\eta = \frac{\sigma_H}{\sigma_{eq}}$  is stress triaxiality where  $\sigma_H$  is hydrostatic stress. The damage in the material is assumed to commence when the state variable  $\omega$  becomes unity defined as:

$$\omega = \int \frac{d\epsilon^p}{\epsilon_f^p(\eta, \epsilon^p)}. \quad (2.3)$$

After onset of damage the stiffness,  $\sigma$ , of failing element is assumed to degrade as:

$$\sigma = (1 - D)\sigma_{eq}. \quad (2.4)$$

where the evolution of damage is governed by the following equation 2.5:

$$\dot{D} = \frac{(L_{eq} \dot{\epsilon}_p)}{\underline{u}_f^p}. \quad (2.5)$$

where,  $L_{eq}$  is the characteristic length of the element while  $\underline{u}_f^p$  is the effective plastic displacement at full degradation/failure.

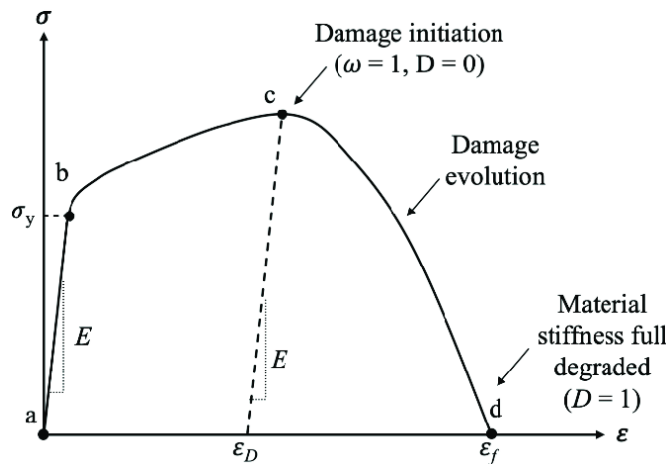


**Fig. 2.1** Typical stress-strain diagram of ductile materials [27].

### 2.1.3 Mohr coulomb plasticity

Mohr-Coulomb plasticity is a classical model describing material deformation, governed by the criterion that failure happens when combined normal and shear stresses reach a critical level. Its yield surface is depicted as an irregular hexagon, with parameters like cohesion and friction angle defining behavior. Widely used in geotechnical and structural engineering for soil analysis, in our simulation we are also modelling soil with the same model.

### 2.1.4 Equation of state

An equation of state (EOS) is a mathematical relationship that describes the thermodynamic properties of a substance, typically in terms of pressure, temperature, and volume. They provide a framework for understanding and predicting the behavior of substances under different conditions, such as phase transitions, compressibility, and thermal expansion. Examples of EOS include the ideal gas law, Vander Waals equation etc. In this study, ideal gas EOS is used to model the air in the atmosphere and JWL EOS is used to model explosives.

#### (i) Ideal gas equation of state

In Abaqus, the Ideal Gas EOS is frequently utilized for modeling blast loading scenarios involving air as the surrounding medium. This equation is applied to replicate the air's response to the high-pressure and high-temperature conditions resulting from an explosion. The Ideal Gas EOS is derived from the foundational Ideal Gas Law, which establishes the interdependence among the gas's pressure (P), volume (V), and temperature (T).

$$PV = nRT \quad (2.6)$$

This EOS is used to model how air experiences rapid compression and expansion caused by blast waves from explosions. It quantifies how pressure, volume, and temperature are interrelated, crucial for accurately predicting how shock waves propagate and interact with structures during simulations. It offers a practical and efficient approach to simulate the dynamic response of air in scenarios involving blast loading. This capability allows one to accurately model and assess how explosions affect structures, thereby assisting in the design of buildings, protective gear, and safety protocols aimed at withstanding blast impacts effectively.

#### (ii) JWL equation of state

The detonation of the charge was approximated through the utilization of programmed burned techniques, while its detonation products were characterized utilizing the Jones-Wilkins-Lee (JWL) equation of state. The Jones-Wilkins-Lee equation of state, also known as JWL, describes the pressure produced during the liberation of chemical energy within an explosive material. This particular model is applied in a programmed burn format, where the reaction and initiation of the explosive substance are not dictated by shock waves within the material. Instead, the initiation timing is established through a geometric arrangement based on the detonation wave velocity and the distance of the material point from the detonation origin.

## 2.2 Finite element (FE) model

The coupled Eulerian-Lagrangian (CEL) approach is a sophisticated numerical method used to simulate how sandwich structures respond to blast loading conditions. In this study, the simulation setup involves a specific configuration to accurately model the interaction between different materials and the blast effects. The schematic of modelling strategy is shown in the Fig. 2.2(a).

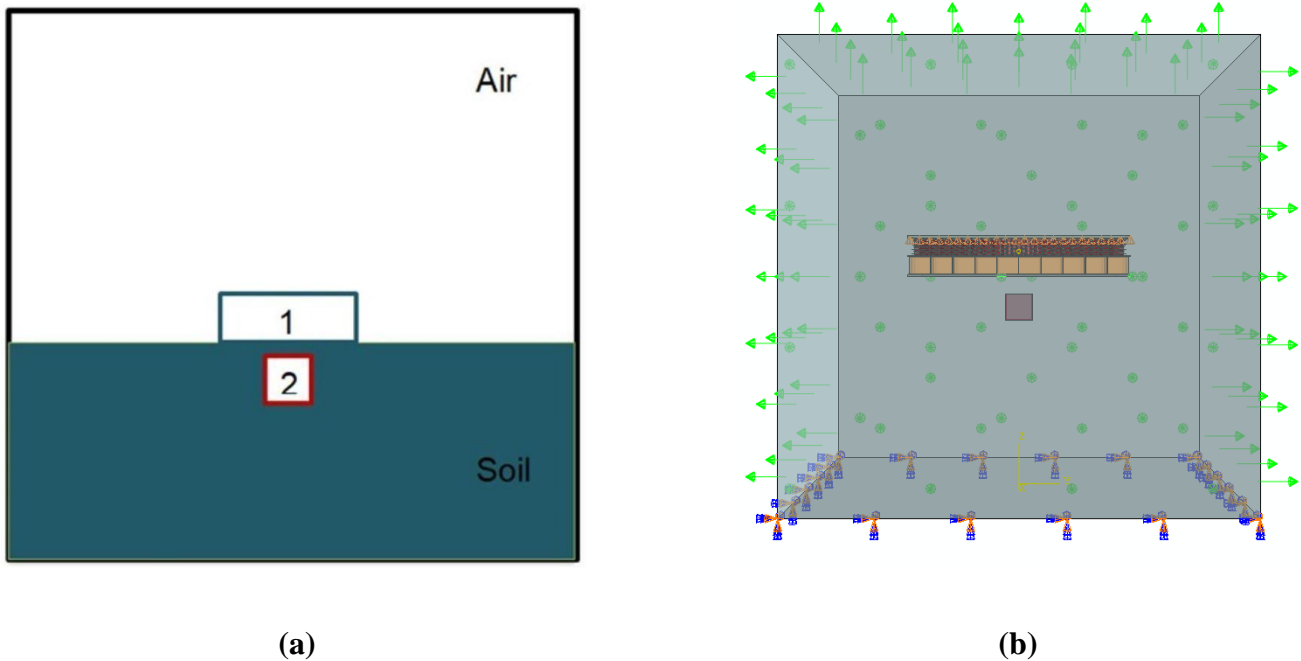


**Fig. 2.2** Modelling strategy (a) Schematic of assembly for finite element simulation, (b) Abaqus Model.

### 2.2.1 Eulerian domain and discretization

The simulation domain is Eulerian in nature, with dimensions of  $0.6 \text{ m} \times 0.6 \text{ m} \times 0.6 \text{ m}$ . This domain is discretized using EC3D8R elements, which are Eulerian 8-node linear brick elements suitable for handling

three-dimensional (3D) simulations in Abaqus. This choice of elements ensures that the domain can accurately capture the deformation and interaction of materials under blast conditions

### 2.2.2 Material distribution

Within the Eulerian domain the distribution is as follows:

**a) Upper Half ( $0.6\text{ m} \times 0.6\text{ m} \times 0.3\text{ m}$ ):** The region indicated by white color in the Fig. 2.2(a) filled with atmospheric air. Air is crucial in blast simulations as it transmits the shock wave and interacts dynamically with other materials.

**b) Lower Half ( $0.6\text{ m} \times 0.6\text{ m} \times 0.3\text{ m}$ ):** The region in dark color as shown in Fig. 2.2(a) represents soil, a solid medium that interacts with the sandwich structure and affects how shock waves propagate through the ground. Soil is typically modeled using Eulerian elements in the CEL approach, allowing it to deform and respond to applied forces realistically.

### 2.2.3 Explosive and structure placement:

A cubical explosive with a side length of 38 mm is inserted into the soil, positioned 25 mm below the bottom surface of the sandwich structure.

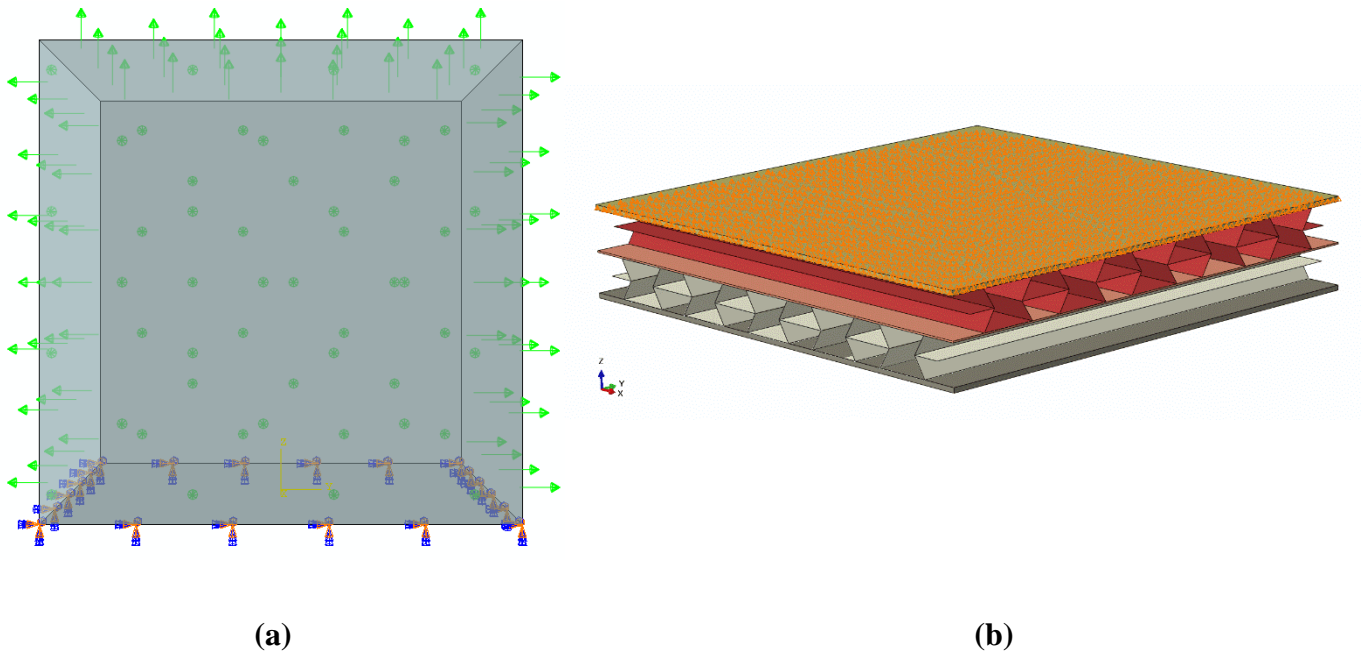


**Fig. 2.3** Boundary conditions of (a) Domain, (b) Structure.

### 2.2.4 Boundary conditions

**a) Eulerian domain:** The bottom surface of the Eulerian domain is constrained to move along all the directions, as shown in Fig. 2.3(a). Other surfaces of the domain are set with outflow nonreflecting conditions, allowing pressure waves to propagate without reflecting back into the simulation domain. This boundary condition is critical for accurately simulating blast wave propagation.

**b) Structural constraints:** Nodes on the top surface of the sandwich structure are constrained to move in the vertical direction as represented in Fig. 2.3(b).

### 2.2.5 FEM model of sandwich structure

The sandwich structure comprises a soft auxetic honeycomb core sandwiched between two plates. The plates are modeled using C3D8R elements, which are 8-node linear brick elements suitable for capturing the structural response. The auxetic honeycomb cells are discretized using S4R elements, which are 4-node linear shell elements appropriate for modeling the geometric and mechanical behavior of the honeycomb structure.

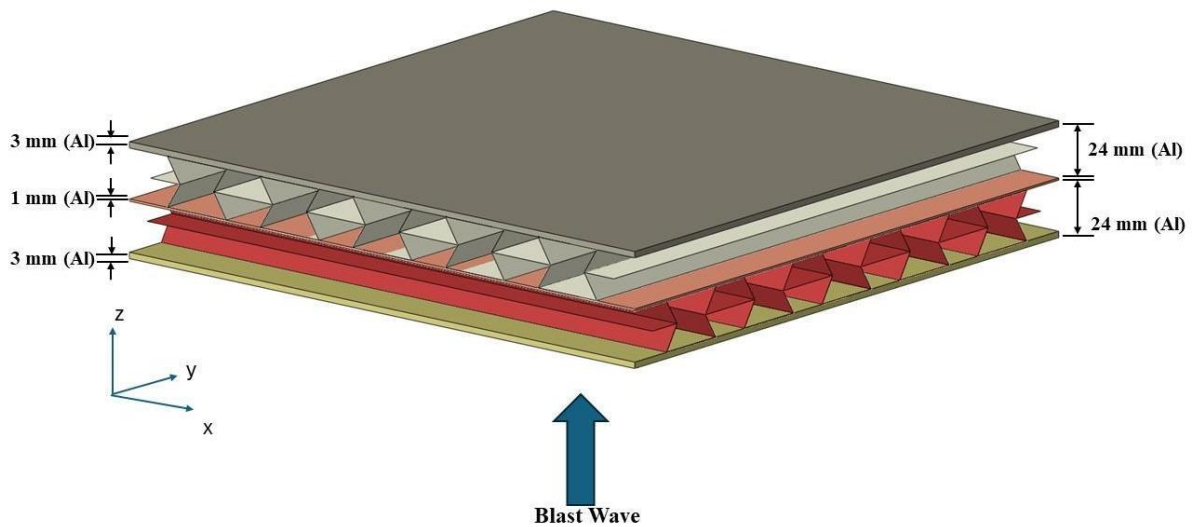


**Fig. 2.4** Blast resistant auxetic honeycomb structure.

The auxetic honeycomb core and face sheets of the sandwich structure require a refined mesh because these regions experience significant deformation and stress concentrations during blast events. Therefore, a very fine meshing (refer Fig. 2.5) with smallest element size (1.5 mm×1.5 mm) is used to discretize the core and face sheets.

### Eulerian domain

The Eulerian domain encompasses the areas surrounding the sandwich structure, including the air above and the soil below. Near the structure, where the explosive is buried and where the air interacts with the top surface of the structure, the mesh resolution needs to be refined. This refinement is necessary to capture the detailed interactions between the dynamic components of the blast event and the solid structure. A finer mesh is required in the immediate vicinity of the structure's surfaces and the explosive (refer Fig. 2.6). This ensures that the simulation accurately captures the shock wave propagation, pressure distribution, and stress concentrations that occur during blast loading. Mesh refinement in these regions allows for precise representation of how energy transfers and interacts between the materials involved.

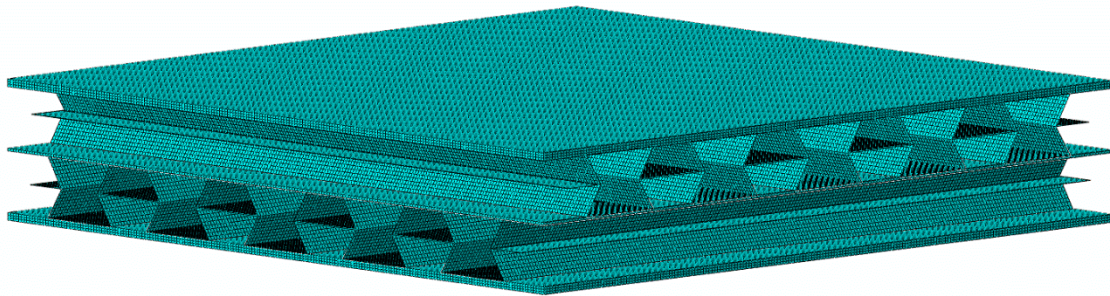


**Fig. 2.5** Finite element model of auxetic honeycomb structure employed in the simulations of blast loading.

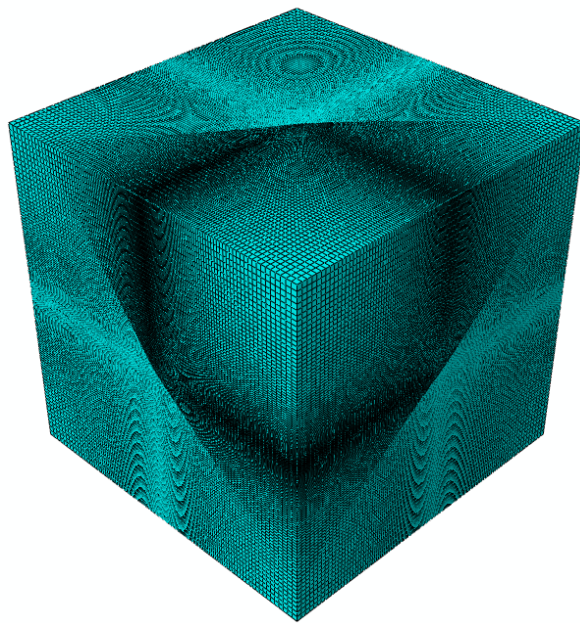


**Fig. 2.6** Finite element model of domain employed in the simulations of blast loading.

In order to study the effect of cell wall thickness on the deformation behavior of sandwich structure, the different values of cell wall thickness (refer Fig. 2.7) of 0.1 mm, 0.5 mm, and 0.75 mm are considered while maintaining a fixed cell size of 24 mm.

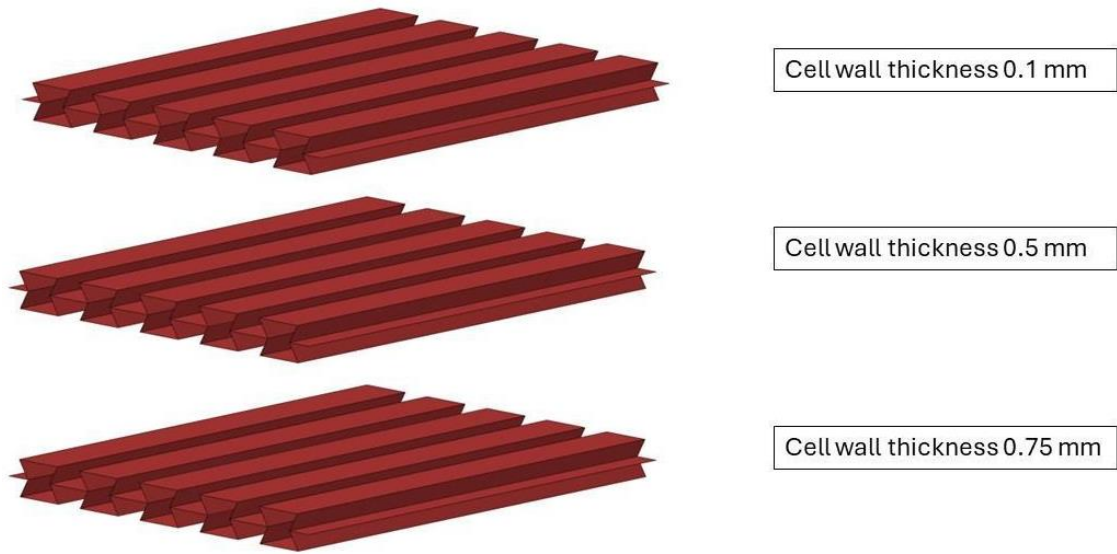


**Fig. 2.7** Variation of cell wall thickness.

Further, the impact of cell size (refer Fig. 2.8) on blast resistance characteristics is investigated by considering cell sizes of 24 mm, 12 mm, and 6 mm for fixed cell wall thickness of 0.75 mm.

In order to understand the effect of loading direction on energy absorption, the simulations are performed by applying blast loading in-plane and out-of-plane of the cells of core (refer Fig. 2.9). This analysis is crucial for optimizing the structure's design to enhance its overall blast resistance and safety.

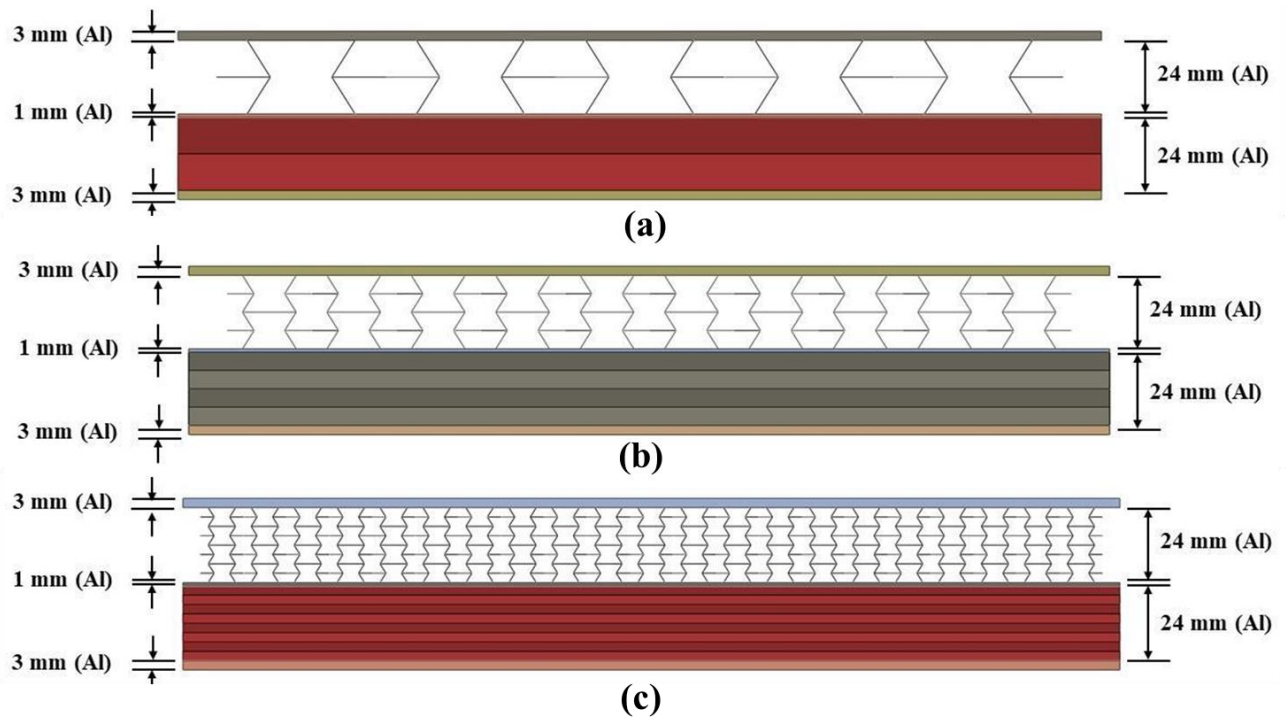


**Fig. 2.8** Varying the size of cell of an auxetic honeycomb (a) 24 mm, (b) 12 mm, (c) 6 mm.

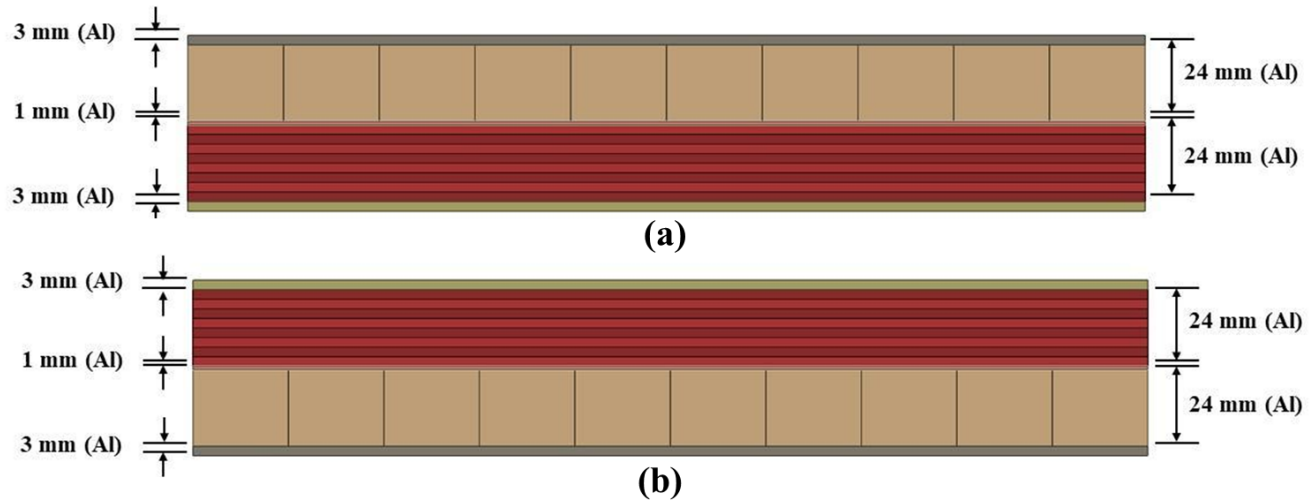


**Fig. 2.9** Different configurations of in-plane and out of plane honeycomb structure (a) Out of plane facing blast , (b) In-plane facing blast.

### 2.3 Material parameters

All the part of the sandwich structure are assumed to be made of an aluminum alloy, which is assumed to follow the constitutive and damage laws of Johnson-Cook [27]. The behavior of soil is assumed to follow the Mohr coulomb plasticity theory. Further, explosive is assumed to be characterized by Jones-Wilkins-Lee (JWL) EOS, while air is assumed to follow Ideal gas EOS. The material constant for aluminum alloy, soil, air and explosive materials are listed in Table. 1-4, respectively.

**Table. 1** Material properties for air taken from [28].

| Eos                              | Air                             |                                  |   |  |
|----------------------------------|---------------------------------|----------------------------------|---|--|
| <b>Gas Constant</b><br>(J /kg K) | <b>Ambient pressure</b><br>(Pa) | <b>Specific Heat</b><br>(J/kg K) | <b>Dynamic Viscosity</b><br>(N s/m <sup>2</sup> ) | <b>Density</b><br>(kg/m <sup>3</sup> ) |
| 287                              | $1.01 \times 10^5$              | $7.18 \times 10^2$               | $1.85 \times 10^{-5}$                             | 1.23                                   |

**Table. 2** Material properties for soil taken from [29].

| Eos                    | Soil             |                 |                 |                       |                    |                |
|------------------------|------------------|-----------------|-----------------|-----------------------|--------------------|----------------|
| <b>Elastic modulus</b> | <b>Poisson's</b> | <b>Friction</b> | <b>Dilation</b> | <b>Cohesion yield</b> | <b>Abs plastic</b> | <b>Density</b> |

|                    |                       |              |              |                    |               |                           |
|--------------------|-----------------------|--------------|--------------|--------------------|---------------|---------------------------|
| <b>(Pa)</b>        | <b>ratio</b>          | <b>angle</b> | <b>angle</b> | <b>stress (Pa)</b> | <b>strain</b> | <b>(kg/m<sup>3</sup>)</b> |
| $5.00 \times 10^7$ | $3.00 \times 10^{-1}$ | 24           | 0.12         | $1.00 \times 10^5$ | 0.00          | $2.20 \times 10^3$        |

**Table. 3** Material properties for TNT taken from [29].

|                                   |   |                           |                      |
|-----------------------------------|---|---------------------------|----------------------|
| <b>JWL</b>                        | <b>TNT</b>                              |                           |                      |
| <b>C<sub>d</sub> (m/s)</b>        | <b>C<sub>1</sub> (Pa)</b>               | <b>C<sub>2</sub> (Pa)</b> | <b>R<sub>1</sub></b> |
| 6930                              | $3.73 \times 10^{11}$                   | $3.74 \times 10^9$        | 4.15                 |
| <b>Density (kg/m<sup>3</sup>)</b> | <b>e<sub>0</sub> (kJ/m<sup>3</sup>)</b> | <b>W</b>                  | <b>R<sub>2</sub></b> |
| $1.65 \times 10^3$                | $6.06 \times 10^6$                      | 0.35                      | 0.9                  |

**Table. 4** Material properties for aluminum taken from [30].

|                                   |                          |                      |  |                          |                      |          |                    |
|-----------------------------------|--------------------------|----------------------|--|--------------------------|----------------------|----------|--------------------|
| <b>Aluminum</b>                   | <b>J-C plastic model</b> |                      | <b>Damage evolution</b>                  |                          |                      |          |                    |
| <b>Young Modulus (Pa)</b>         | <b>Poisson's ratio</b>   |                      | <b>Fracture energy (J/m<sup>2</sup>)</b> |                          |                      |          |                    |
| $7.00 \times 10^{10}$             | 0.3                      |                      | 2630009                                  |                          |                      |          |                    |
| <b>A (Pa)</b>                     | <b>B (Pa)</b>            | <b>N</b>             | <b>T<sub>m</sub> (K)</b>                 | <b>T<sub>r</sub> (K)</b> | <b>M</b>             | <b>C</b> | <b>Strain rate</b> |
| $5.2 \times 10^8$                 | $4.77 \times 10^8$       | 0.52                 | 893                                      | 293                      | 1                    | 0.001    | 0.0005             |
| <b>Density (kg/m<sup>3</sup>)</b> | <b>D<sub>1</sub></b>     | <b>D<sub>2</sub></b> | <b>D<sub>3</sub></b>                     | <b>D<sub>4</sub></b>     | <b>D<sub>5</sub></b> |          |                    |
| $2.70 \times 10^3$                | 0.096                    | 0.049                | 3.465                                    | 0.016                    | 1.099                |          |                    |

# Chapter 3

## Result and discussion

### 3.1 Effect of cell wall thickness

Figs. 3.1(a)-(c) show contour plots of equivalent plastic strain at time of 0, 0.075 and 0.15 ms for structure having cell wall thickness of 0.1 mm. The corresponding plots for cell wall thickness 0.5 and 0.75 mm are shown in Figs. 3.1(d)-(f) and (g)-(i), respectively.

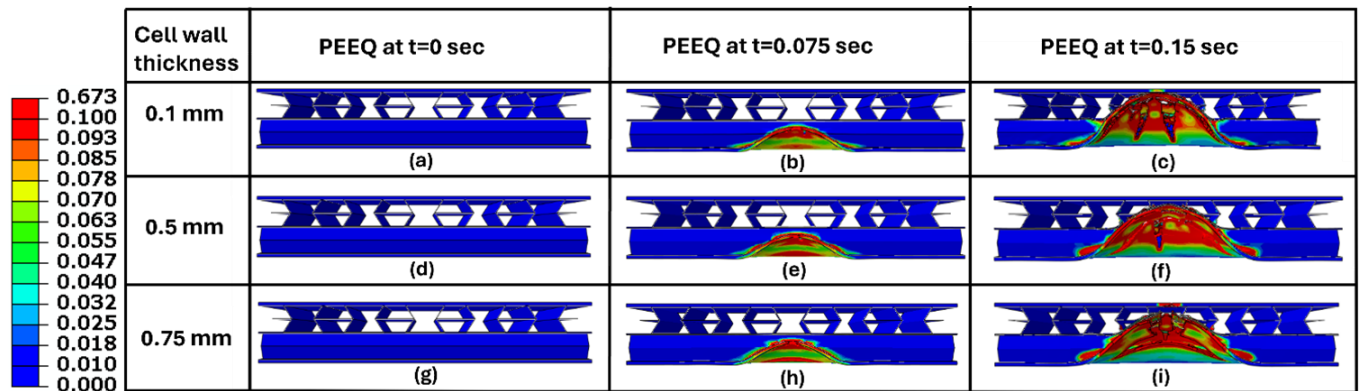


**Fig. 3.1** Evolution of damage for different cell wall thickness structures.

The evolution of energy absorbed by the structure and pressure on top surface of upper plate are displayed in Fig. 3.2 and Fig. 3.3, respectively, for different cell wall thickness. It can be noticed from these figures that absorbed energy as well as pressure on top surface increases with increase in cell wall thickness. However, after complete crushing of 0.1 mm thick cells, pressure rises steeply. Thus, pressure attenuation is higher in structure with thinner cell walls. This is due to the fact that the strength of honeycomb decreases with reduction in cell wall thickness resulting in drop in the resistance to deformation. Therefore, the structures with thinner cell walls deform easily and attenuate the pressure very effectively, but energy absorption drops at the cost of better pressure attenuation provided by thinner honeycombs.

### 3.2 Effect of cell size

Figs. 3.4(a) – (c) contrast the evolution of plastic strain or deformation in structures having different sizes of cell. It can be seen that deformation is distributed to a greater number of cells in structure with smaller cell size in contrast to the structure with bigger cell size. From Fig. 3.5, it is evident that the energy absorption also the duration that structure can sustain blast is also found to be increased, From Fig. 3.6. It can be interpreted that with decrease in cell size the pressure on the top surface of the structure decreases, it can be

conclude that with decreasing the cell size i.e., by increasing the number of cells the blast carrying capacity of the structure increases by the structures increases with decrease in size of cell. Although with decrease in cell size the structure was able to sustain the blast for longer duration.

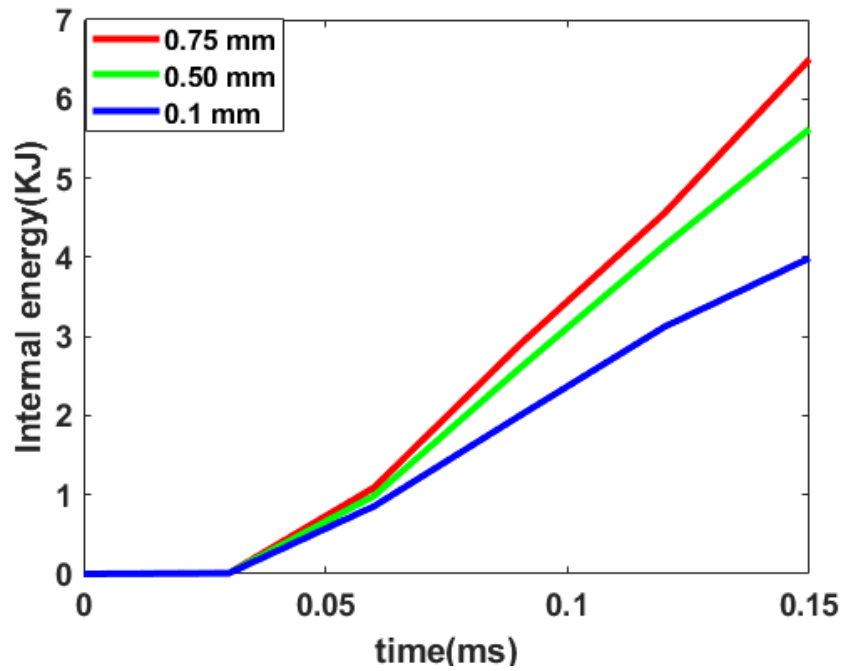


Fig. 3.2 Evolution of energy absorption for different cell wall thickness.

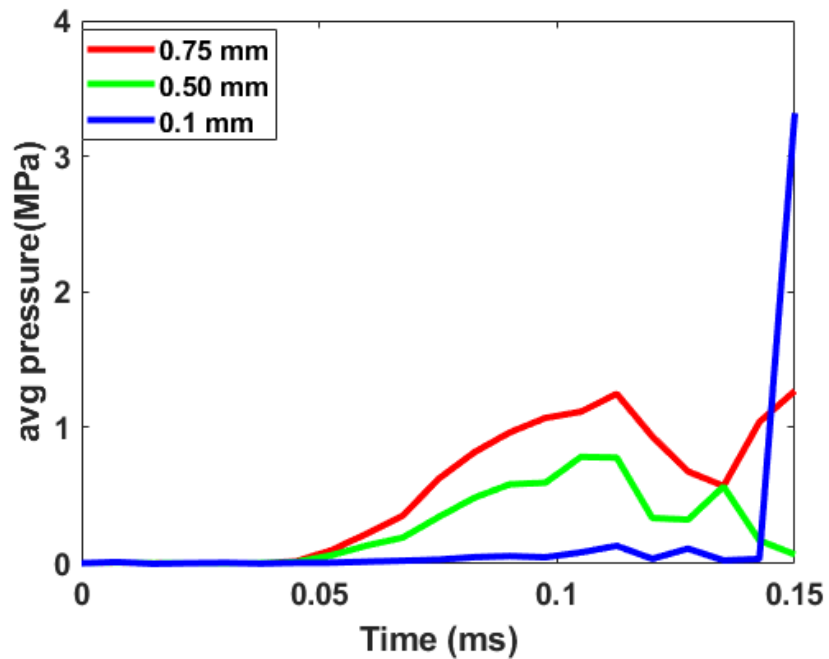
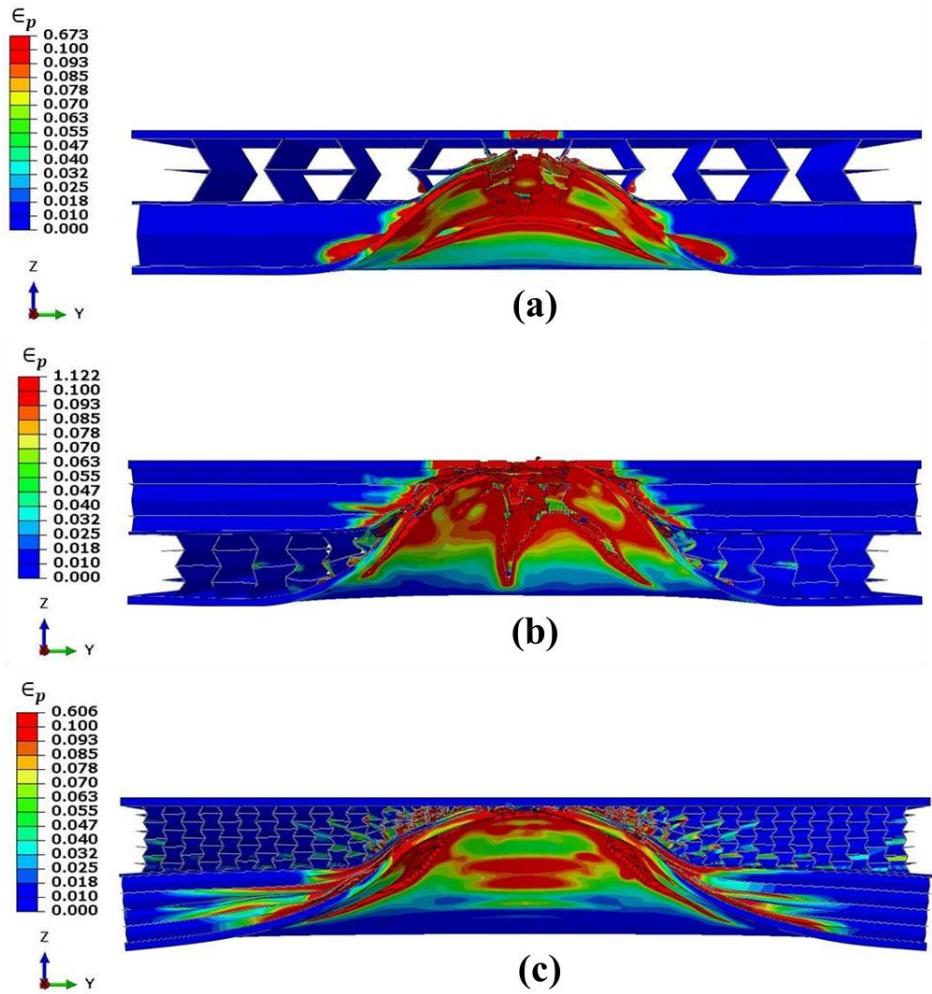
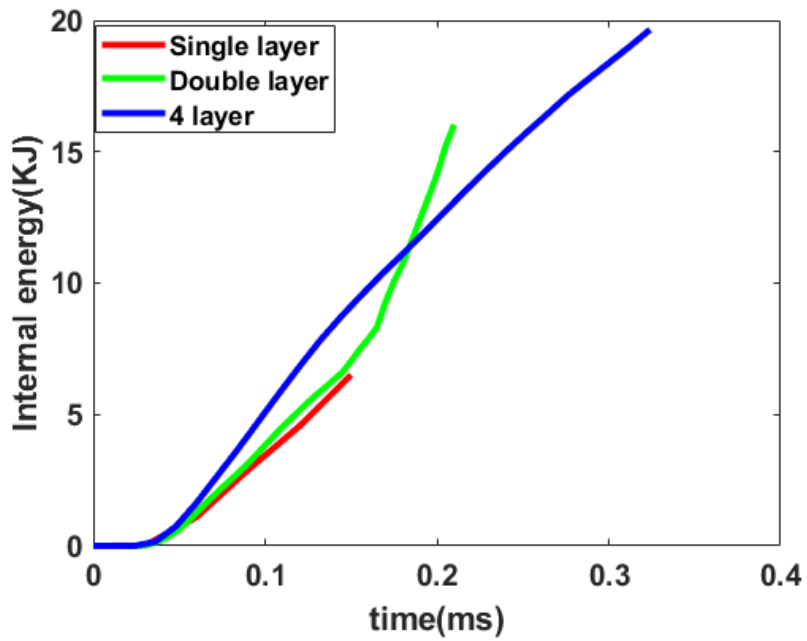


Fig. 3.3 Evolution of pressure on the top surface of structure for different cell wall thicknesses.



**Fig. 3.4** Contour plots of equivalent plastic strain for different cell size; (a) 24 mm, (b) 12 mm, (c) 6 mm.



**Fig. 3.5** Evolution of energy absorption for different cell size honeycomb structures.

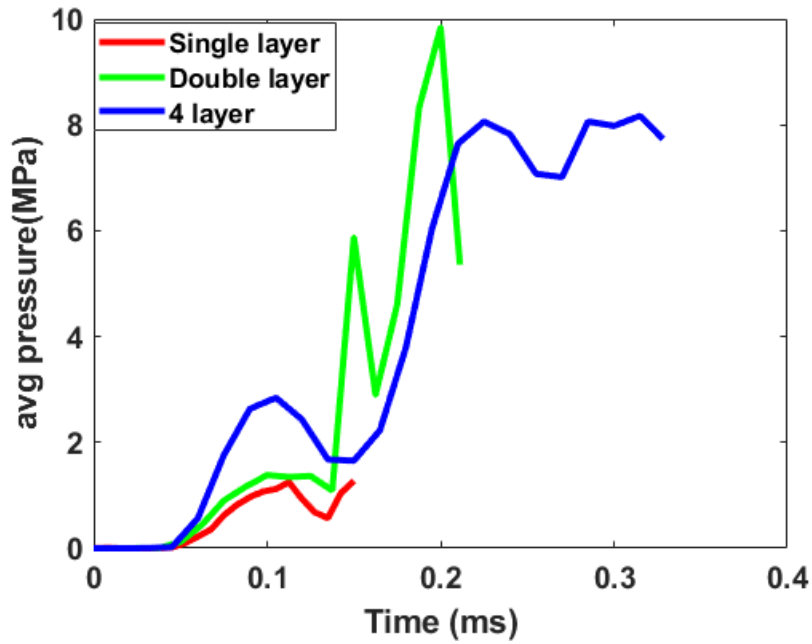


**Fig. 3.6** Evolution of pressure on the top surface for different cell size honeycomb structures.

### 3.3 Effect of combining in plane and out of plane

Based on the previous results, the best cell wall thickness (0.75 mm) and cell size (6 mm) were used for further simulations, in order to get best performance among the available structures. The structures consisting of combination of in-plane and out-of-plane honeycombs were subjected to near field blast loading and the following observations can be made from the Fig. 3.7(a) that when the in-plane honeycomb structure is placed towards the blast side then more uniform deformation takes place in the structure, while in second case when out-of-plane honeycomb is placed towards the blast side it suffers localized deformation at the center area, as the consequence of above the structure in which in-plane honeycomb is placed at blast side, dissipates more energy than the structure in which out-of-plane honey comb is placed on blast side. It can be inferred from Fig. 3.8 and Fig. 3.9 that there is an enhancement in energy absorption along with a reduction in peak overpressure. An analysis has been conducted to determine the significant impact of the arrangement of such a composite structure on energy absorption and peak pressure. The peak pressure experienced in the out-of-plane orientation during a blast event was found to be 3.8% lower than that in the in-plane orientation, with a corresponding 15% decrease in energy absorption.

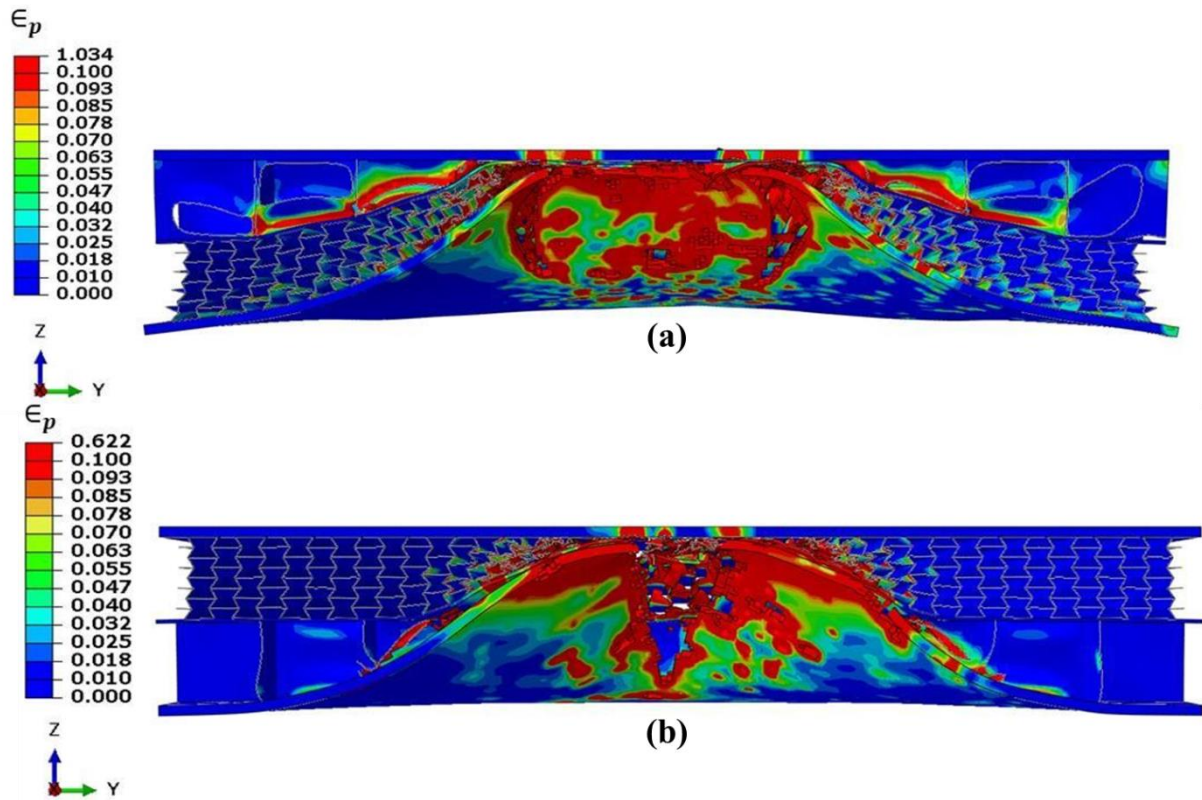


**Fig. 3.7** Contour plots of equivalent plastic strain for (a) In-plane honeycomb on blast side, (b) Out-plane honeycomb on the blast side.

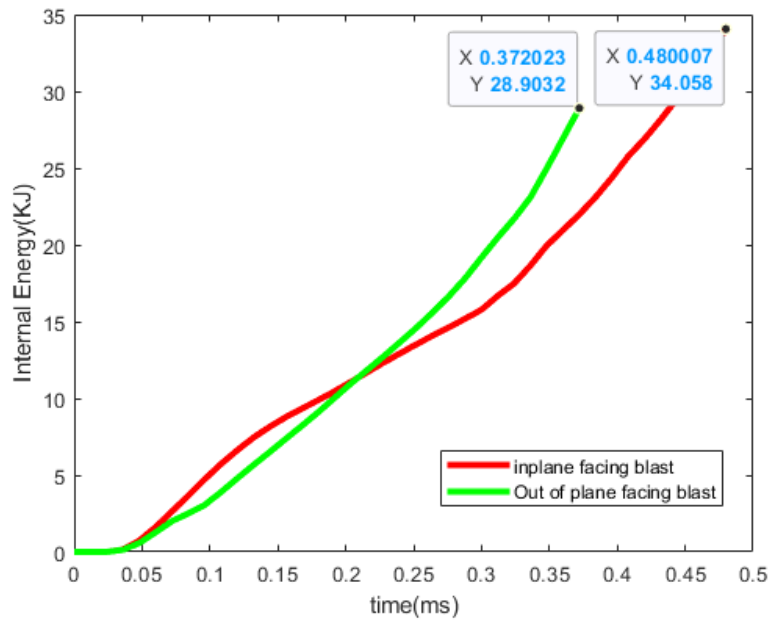


**Fig. 3.8** Energy absorption for in plane and out of plane combined with one of them facing blast side.

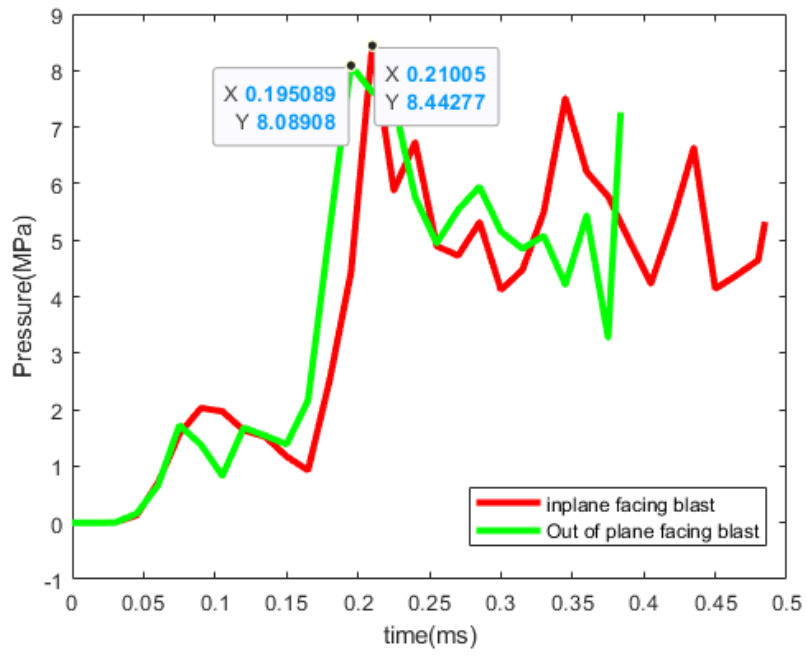


**Fig. 3.9** Pressure variation for in plane and out of plane combined with one of them facing blast side.

# Chapter 4

## Conclusion and future scope

### 4.1 Conclusions

The finite element simulation of sandwich honeycomb structures subjected to near field blast loading were performed using coupled Eulerian-Lagrangian technique available in commercially available software package abaqus 2017 and the effects of cell wall thickness and number of cells on the energy absorption and pressure attenuation capabilities on the structure are investigated. In addition, the combination of in plane and out of plane loading on the blast resistant capability is analyzed. The important results from the present study are as follows:

- It can be concluded that the thinner shells attenuate the pressure effectively but conversely absorb lesser energy. Also, thinner shells cannot sustain blast wave for longer duration, therefore an optimum thickness has to be chosen.
- The pressure attenuation and energy absorption increase with decrease in cell size. Combinations of in-plane and out of plane honeycombs are found to be much more effective in pressure attenuation and energy absorption in comparison to the structure with in-plane loading only.
- Further the sequence of in plane and out of the plane honeycomb also investigated, although significant difference is not observed in pressure attenuation but considerable energy absorption increment has been found in case of in plane honeycomb facing the blast.

### 4.2 Future scope of work

- i. Further optimization can be done in order to increase the energy absorption with other available structures and different structures like origami can also be explored.
- ii. One can test the efficacy of multiple layers of auxetic structures in reducing pressure transmission to 6.2 MPa, potentially outperforming other core materials in terms of blast resistance.
- iii. The results obtained in the thesis yet needs to be experimentally validated; therefore the experiments of blast loading on the sandwich structure with suggested design can be performed.

## References

- [1] Li, Zongwen, and Jianxun Ma. "Experimental study on mechanical properties of the sandwich composite structure reinforced by basalt fiber and nomex honeycomb." *Materials* 13.8 (2020): 1870.
- [2] Jakubczak, Patryk, et al. "Experimental investigation on the low velocity impact response of fibre foam metal laminates." *Materials* 14.19 (2021): 5510.
- [3] Huo, Xintao, et al. "On low-velocity impact response of foam-core sandwich panels." *International Journal of Mechanical Sciences* 181 (2020): 105681.
- [4] <https://topolocfrt.com/aluzinc-sandwich-panels/>
- [5] Sun, Guangyong, et al. "On the structural parameters of honeycomb-core sandwich panels against low-velocity impact." *Composites Part B: Engineering* 216 (2021): 108881.
- [6] Zou, Z., et al. "Dynamic crushing of honeycombs and features of shock fronts." *International Journal of Impact Engineering* 36.1 (2009): 165-176.
- [7] Theobald, M. D., et al. "Large inelastic response of unbonded metallic foam and honeycomb core sandwich panels to blast loading." *Composite structures* 92.10 (2010): 2465-2475.
- [8] Thomas, Tiju, and Gaurav Tiwari. "Performance evaluation of Reinforced honeycomb structure under blast load." *Journal of Engineering Research* 11.1B (2023).
- [9] Li, Meng, et al. "Optimizing crashworthiness design of square honeycomb structure." *Journal of Central South University* 21 (2014): 912-919.
- [10] Sahu, Santosh Kumar, PS Rama Sreekanth, and SV Kota Reddy. "A brief review on advanced sandwich structures with customized design core and composite face sheet." *Polymers* 14.20 (2022): 4267.
- [11] Zhu, Yilin, et al. "In-plane elastic properties of a novel re-entrant auxetic honeycomb with zigzag inclined ligaments." *Engineering Structures* 268 (2022): 114788.
- [12] Tarlochan, Faris. "Sandwich structures for energy absorption applications: A review." *Materials* 14.16 (2021): 4731.
- [13] Lestari, Ary, et al. "Ceramic Armor as Protective Material in Defense Industry Product: A Literature Review." *MOTIVECTION: Journal of Mechanical, Electrical and Industrial Engineering* 5.1 (2023): 101-112.
- [14] Joshua, J. J. J., et al. "Fabrication and Experimental Estimation of Mechanical Properties of Kevlar-Glass/Epoxy Interwoven Composite Laminate." *Journal of Nanomaterials* 2023.1 (2023): 1055071.
- [15] Ruan, Fangtao, et al. "Bending and Impact Performance of Kevlar/Basalt Fabric Interlayer Hybrid Curved Composites." (2022).

- [16] Qi, Chang, et al. "Ballistic resistance of honeycomb sandwich panels under in-plane high-velocity impact." *The Scientific World Journal* 2013 (2013).
- [17] Wang, Yuanlong, et al. "On the out-of-plane ballistic performances of hexagonal, reentrant, square, triangular and circular honeycomb panels." *International Journal of Mechanical Sciences* 173 (2020): 105402.
- [18] Guo, Guodong, Shah Alam, and Larry D. Peel. "Numerical analysis of ballistic impact performance of two ceramic-based armor structures." *Composites Part C: Open Access* 3 (2020): 100061.
- [19] Verma, Karan Singh, et al. "Influences of cell size, cell wall thickness and cell circularity on the compressive responses of closed-cell aluminum foam and its FEA analysis." *International Journal of Metalcasting* 16.2 (2022): 798-813.
- [20] Yazici, Murat, et al. "Experimental and numerical study of foam filled corrugated core steel sandwich structures subjected to blast loading." *Composite structures* 110 (2014): 98-109..
- [21] Bonorchis, D., and G. N. Nurick. "The influence of boundary conditions on the loading of rectangular plates subjected to localised blast loading—importance in numerical simulations." *International Journal of Impact Engineering* 36.1 (2009): 40-52.
- [22] Nurick, G. N., M. E. Gelman, and N. S. Marshall. "Tearing of blast loaded plates with clamped boundary conditions." *International journal of impact engineering* 18.7-8 (1996): 803-827.
- [23] Michalski, Jakub, and Tomasz Streck. "Blast resistance of sandwich plate with auxetic anti-tetrachiral core." *Vibrations in Physical Systems* 31.3 (2020).
- [24] Bahei-El-Din, Yehia A., and George J. Dvorak. "Enhancement of blast resistance of sandwich plates." *Composites Part B: Engineering* 39.1 (2008): 120-127.
- [25] Ahmed, Sameh, and Khaled Galal. "Effectiveness of FRP sandwich panels for blast resistance." *Composite Structures* 163 (2017): 454-464.
- [26] Karahan, Mehmet, and Nevin Karahan. "Development of an innovative sandwich composites for the protection of lower limbs against landmine explosions." *Journal of Reinforced Plastics and Composites* 35.24 (2016): 1776-1791.
- [27] Farahani, H. K., Mostafa Ketabchi, and Sh Zangeneh. "Determination of Johnson–Cook plasticity model parameters for Inconel718." *Journal of Materials Engineering and Performance* 26 (2017): 5284-5293.
- [28] Mokhtari, M., and A. Alavi Nia. "The application of CFRP to strengthen buried steel pipelines against subsurface explosion." *Soil Dynamics and Earthquake Engineering* 87 (2016): 52-62.
- [29] Lu, Gongda, and Mamadou Fall. "State-of-the-art modelling of soil behaviour under blast loading." *Geotechnical and Geological Engineering* 36 (2018): 3331-3355.

[30] Žmindák, Milan, et al. "Finite element modelling of high velocity impact on plate structures." Procedia Engineering 136 (2016): 162-168.